

Fluctuations in annual cycles and inter-seasonal memory in West Africa: rainfall, soil moisture and heat fluxes

Bernard Fontaine*, Samuel Louvet* and Pascal Roucou*

* Centre de Recherches de Climatologie, UMR5210, CNRS / University of Burgundy, Dijon, France

Contact: B. Fontaine, Centre de Recherches de Climatologie, UMR5210, CNRS / University of Burgundy, Bât Sciences Gabriel, BP, 21004 Dijon Cedex, France.

(Email: bernard.fontaine@u-bourgogne.fr).

Summary:

Annual cycle and inter-seasonal persistence of surface-atmosphere water and heat fluxes are analyzed at a 5-day time step over the West African Monsoon (WAM) through observational precipitation estimates (CMAP), model datasets (NCEP/DOE level 2 reanalyses) and a Soil Water Index (SWI) from the ERS scatterometer. Coherent fluctuations (30-90 days) distinct from supra-synoptic variability (10-25 day periods) are first detected in the WAM precipitation and heat fluxes over the period 1979-2001. During all the northward excursion of the WAM rain band, a succession of four active phases (abrupt rainfall increases) occurs. They are centered in the first days of March, mid-April, the second half of May and from the last week of June to mid-July (the Sahelian onset). A simple statistical approach shows that the Spring to Summer installation of the monsoon tends to be sensitive to these short periods. Other analyses suggest the existence of lagged relationship between rainfall amounts registered in successive Fall, Spring (active periods) and Summer (top of the rainy season) implying land surface conditions. The spatial extension of the generated soil moisture anomalies reaches one maximum in March, mainly at the Guinean latitudes and over the Sahelian belt where the signal can persist until the next monsoon onset.

Typically after abnormal wet conditions in September-October two signals are observed: (1) more marked fluctuations in Spring with less (more) Sahelian rainfall in May (June and after) at the Sahelian-Sudanian latitudes; (2) wetter rainy seasons along the Guinean coast (in Spring and Summer with an advance in the mean date of the 'little dry season'). The reverse arises after abnormal dry conditions in autumn.

I. Introduction

Annual cycle and interannual to decadal rainfall fluctuations over West Africa and their association with the Sea Surface Temperature (SST) variability have been noted for a long time, first over the Atlantic Ocean and then at a quasi-global scale. It is clear that part of monsoon variability responds to external forcing, e.g. SST anomaly patterns of quasi-global or more regional scales. However, since the seminal works of Charney (1975, 1977), many numerical experiments (for example in Zeng et al., 1999 and Wang and Eltahir, 2000) have recognized the role of land surface as a major and dominant factor at local and meso scales in spatial distribution of rain events. In this context, a lot of numerical studies have first focused on the close relationship linking soil moisture and precipitation mainly at the interannual time scale (Xue and Shukla, 1993). The strong interannual persistence of rainfall anomalies has been explained in terms of land-surface feedback due to the slow

adjustment time of soils covered by vegetation south of Sahel (Zeng and Neelin, 2000). Eltahir and Gong (1996) and Cook (1999) emphasized the role of the meridional moist static energy (MSE) and thermal gradients in low levels for WAM dynamics whereas Fontaine et al. (1999) pointed out the dominant role of Spring to Summer changes in MSE gradients for seasonal rainfall forecasting in West Africa. More recently, numerical (Douville and Chauvin, 2000) and empirical (Philippon and Fontaine, 2002) studies have focused on the relevance of soil moisture for seasonal prediction. The latter authors have observed that abnormally wet Sahelian rainy seasons tend to be preceded by abnormally wet soils over the Sudanian-Guinean belt in northern Fall suggesting the possible existence of an in situ long-term memory controlled by soil moisture. However, using a simple water model Shinoda and Yamaguchi (2003) conclude that the root-zone soil moisture does not act as a memory of Sahelian rainfall anomaly into the following rainy season and cannot be directly related to the long-term persistence of the drought.

The purpose of this study is to document the West African long-term memory, (i.e., abnormally wet Sahelian rainy seasons tend to be preceded by abnormally wet soils and rainfall over the Sudanian-Guinean belt during northern Fall), in terms of rainfall annual cycle and variability during the northward excursion of the WAM system in northern Spring. We will focus on the water and heat exchanges on the continent, since over ocean, surface-atmosphere interactions are triggered by the positive feedbacks in the strong coupled SST-wind system over the eastern equatorial Atlantic (Mitchell and Wallace, 1992) and the air-sea coupling through vertical air-sea fluxes is more important at a decadal scale (Chang et al., 1997) than at a seasonal or intra-seasonal scale (Li and Philander, 1997). By contrast, over land they are more due to varying land surface parameters such as vegetation and soil moisture which control locally the vertical heat and water fluxes.

A few recent studies have been devoted to the installation of the WAM system with an intra-seasonal approach. Grodsky and Carton (2001) and Louvet and Janicot (2003) have detailed the “pre-onset” and “onset” of the first Guinean rainy season while Sultan and Janicot (2000), Janicot and Sultan (2001), and Sultan et al. (2003) focused on the abrupt latitudinal shift of the rain band over the Sahel and associated signals in moisture advection, atmospheric dynamics and convection. Matthews (2000 and 2004) proposes an interesting hypothesis in which intra-seasonal fluctuations arise partly as a remote response to the 30-60 day Madden-Julian oscillations over the warm pool sector: the equatorial Kelvin wave

response to this change propagates eastward and an equatorial Rossby wave response propagates westward. After a complete circuit of the equator they meet up twenty days later over Africa, where the negative mid-tropospheric temperature anomalies in the Kelvin and Rossby wave can favour deep convection. More recently, Louvet et al. (2003) have shown, through analyses of the CMAP dataset, that the different monsoon stages considered above (i.e, the Guinean pre-onset and onset, the Sahelian latitudinal shift of the rain band) are neither specific to a given latitudinal zone nor independent. They occur at the end of periods of pause in rainfall during the northward excursion of the rainbelt and could impact on the future rainy season.

So, rainfall over the WAM region appears to be controlled by long-term memory processes which explain part of the quasi decadal and interannual variability of the cumulative amounts registered during a rainy season. Nonetheless, there is no clear physical link between this large scale memory and the successive rain events of meso scale (i.e., squall lines, convective systems) or of synoptic scale. In this context variability during the northward excursion of the WAM system is important to consider because it impacts directly the dates of onsets and the length of the rainy seasons. We make the hypothesis that a significant part of rainfall in northern Spring is sensitive to the continental amounts registered during the preceding monsoon withdrawal, the other part responding to external forcing, often of oceanic origin (e.g. SSTs).

By contrast with Louvet et al. (2003) who documented the periods of pauses, we will focus on the active phases to detect critical periods during all the northern excursion of the WAM system. Recent availability of latest version of the NCEP/DOE reanalyses level II, the CPC Merged Analysis of Precipitation (CMAP) and Soil Moisture Archive from ERS Scatterometer data offers such an opportunity at the very beginning of the 2006-2007 AMMA field experiments.

II. The data

Rainfall data from CMAP are used in a version where observations from raingauges have been merged only with estimates from infrared and microwave data from satellites then analyzed on a 2.5 x 2.5 degree latitude/longitude grid. The data, available at a 5-day time-scale over the period 1979-2001, depend mainly on observations since rainfall forecasts from the model are not assimilated in the selected CMAP version. The technique and algorithms

are described in Spencer (1993) and Xie and Arkin (1997). It is noteworthy that this version is very close to the *in situ* daily rainfall amounts over the continent both in rhythm (linear correlation coefficients) and in amplitude (means and standard deviations) as shown in the Table 1 of Louvet et al. (2003) for the rainfall estimates compiled by IRD (Institut de Recherche pour le Développement), ASECNA (Agence pour la Sécurité de la Navigation Aérienne en Afrique et à Madagascar) and CIEH (Comité Inter-africain d'Etudes Hydrauliques) after interpolation on the $2.5^\circ * 2.5^\circ$ grid and calculation of 5-day averages .

To describe the surface-atmosphere heat fluxes we have chosen the NCEP/DOE AMIP-II Reanalysis (R-2) because for this version of reanalysis, model precipitation has been replaced with observed (satellite + gauge) 5-day precipitation in a similar manner to CMAP and in the same spatial resolution (Kanamitsu et al., 2002). Moreover R-2 improves upon the NCEP/NCAR Reanalysis(R-1) by fixing the errors and by updating the parameterizations of the physical processes. However no direct assimilation of radiances, but (proper) use of SSM/I data and assimilation of rainfall data have been incorporated. The main improvements regarding the water cycle, as well as the effect of satellite and aircraft, on analyses are extensively discussed in Kanamitsu et al. (2002), in particular the correction method equivalent to using observed 5-day precipitation amounts in the hydrological calculations. Maurer et al. (2001) found that R-2 provides more accurate pictures of soil wetness, near surface temperature and surface hydrology budget over land, and radiation fluxes over Ocean. By contrast the new boundary layer and convection schemes have modified the water vapor profile: R-2 has more moisture in low levels than R-1. In any case, over the West African continent the atmospheric and surface variables or parameters are more accurate; surface albedo over the Sahara goes also from 0.3 in R-1 to beyond 0.4 in accordance with observations.

Considering these aspects we will focus only on the surface parameters that are most closely linked to the water cycle over land at regional scale: i.e., the observed rainfall amounts and reanalyzed sensible and latent heat fluxes at a 5-day time-step over the period 1979-2001. We define first a West African Monsoon area (WAM: $5^\circ\text{-}20^\circ\text{N}$; $10^\circ\text{W}\text{-}10^\circ\text{E}$): this domain is very representative and concentrates the major part of the synoptic disturbances, organized convective and rainy systems (i.e, squall lines). The WAM box is then divided into three equal basic zones of 5° extension: a 'Sahelian' zone (SAH: $15^\circ\text{N}\text{-}20^\circ\text{N}$) a 'Sudanian' zone (SUD: $10^\circ\text{N}\text{-}15^\circ\text{N}$) and a 'Guinean' zone (GUI: $5^\circ\text{N}\text{-}10^\circ\text{N}$).

Additionally, an independent dataset, the soil water index (SWI) from the Global Soil Moisture Archive 1992-2000 from ERS Scatterometer Data, has been retained for studying the land surface evolution. Indeed, SWI is not a direct measurement of soil moisture content but a satellite estimate based on the backscatter coefficient from the ground surface. Each SWI is expressed in percentages (relative measure) ranging between 0 (dry soil) and 1 (100% saturated soil). In fact the scatterometer estimates the top soil moisture (approximately the upper 5 centimetres of the soil) and calculation of SWI is based on this measurement for depicting the available water content in the rooting zone. SWI is influenced by vegetation and surface roughness, so methods have been developed to eliminate these effects (see for details, Wagner and Scipal, 2000 and Wagner et al., 1999). However such techniques allow derivation of the soil moisture content at a regional scale (50 km) through the conductivity of the top soil, at a time sampling of 1-2 observations per week over Africa. At this frequency the SWI depicts mainly the available top-soil water content. For the West African region there are 10,218 SWI estimates available at a ten-day time step over the period 1992-2000 (see for example graphs in Figures. 5 a, b and maps in Figures. 6b-d).

III. Mean annual cycles and fluctuations

Figure 1 presents mean annual evolutions of filtered rainfall records (RR), their time tendencies and the sensible (H), latent (LE) and total (H+LE) heat fluxes at the surface over the three latitudinal bands. It is noteworthy that RR is a filtered ‘observed’ signal after elimination of fluctuations < 5 pentads (30 days) by a low-pass butterworth filter (Murakami, 1979, while H and LE are ‘raw model products’ which reflect how the NCEP model deals with soil moisture holding capacity. Over the Sahel (Fig.1 a-c) RR, LE and H+LE reach their annual maximum in the second part of August following the annual maximum in H which occurs by the end of June in clear concomitance with the beginning of the rainy season as shown by the sudden rainfall increase called ‘Sahelian onset’ in Figure. 1b. Over the Sudanian belt (Fig. 1d-f) the shapes of RR, H and LE differ: RR peaks also in August but the total heat flux remains nearly constant ($> 110 \text{ W/m}^2$) -from April when H reaches its first peak to October when LE starts its decrease-. Here also the H peak is clearly concomitant with the beginning of rainy season (Fig. 1d). It is noticed that from April to July the Sudanian belt (Fig. 1e) is marked by recurrent a succession of abrupt increases observed in 2/3 of years which indicates the phase-locking to the annual cycle (black bars). These ‘active periods’ are

followed by short pauses (attenuations). At Guinean latitudes, rainfall amounts peak in June and September (Fig. 1g) according to the double annual displacement of the Solar apparent position and rain belt and exhibits similar active periods with less phase-locking. The LE flux remains nearly constant all along the year ($80-100 \text{ W/m}^2$) and the H cycle is mono-modal and peaks in February (Fig. 1i).

Mean rainfall tendencies prove that the Spring to Summer installation of the monsoon is neither continuous nor linear but tends to be concentrated on specific short periods of the year. More precisely, there are four preferential periods of rainfall increase in West Africa: 1) the turn of February/March in the Guinean latitudes, 2) mid-April, 3) the end of May over the whole Guinean-Sudanian area, and 4) the turn of June/July over the Sudanian-Sahelian belt, which corresponds to the monsoon onset. However, these active phases can be affected by shorter fluctuations, as shown in Figure 2: if some peaks refer to the 13-16 and 20-25 day periods (linked to supra-synoptic variations), variations > 30 days (called hereafter intra-seasonal) appear clearly more energetic and significant. Such variations can be induced by a large number of mechanisms linked to either internal atmospheric dynamics of synoptic scale (a few days) or climate mechanisms of longer periods due to interactions with the oceanic and land surfaces (Grodky and Carton, 2001; Sultan and Janicot, 2000, 2003; Louvet and Janicot, 2003).

The four abrupt rainfall increases can be viewed as periods of greater occurrence of monsoon surges in the West African monsoon during its northward penetration into the continent. This is well illustrated in Figure 3 which illustrates also the discontinuous shape of rain band and alternation in active phases and pauses from March to July. The mean annual evolution is rather simple. The first Guinean rainy season ($> 6 \text{ mm/day}$ south of 7°N in June) occurs after the total heat flux annual peak in February-March ($> 130 \text{ W/m}^2$ at $6-7^\circ\text{N}$ in Fig. 3b) which precedes a rapid increase in sensible heat flux over $10-15^\circ\text{N}$ in March-April (Fig. 3c). In Summer the core of the Sudanian-Sahelian rain belt ($> 7 \text{ mm/day}$ at $8-12^\circ\text{N}$) is located just southward to the heat belt (H+LE maximums $> 120 \text{ W/m}^2$ at $13-15^\circ\text{N}$ in Figure. 3b) leading the annual peak in LE flux ($> 110 \text{ W/m}^2$ in October-November, Fig. 3d).

So the mean annual cycle of the West African monsoon cannot be reduced to a continuous latitudinal excursion of the rain band following the solar declination. It appears associated with two types of surface forcing which are largely out of phase: sensible energy north of 10°N (Fig. 3c) just before the first rainfall maximum over 'Sudan-Sahel' and latent energy in

Autumn south of 10°N (Fig. 3d) after the second RR maximum during the monsoon withdrawal. In Spring, energy is pumped from the surface mainly through sensible-heating and is driving convection northward (Fontaine et al., 2002), but latent energy depends on the available soil moisture and is hence stronger during the second Guinean rainy season.

The correlation coefficients between the first three active phases (AP #1,2,3) over the ‘Sudan-Sahel’ region (10°N - 18.5°N ; 10°W - 10°E) and the 5-day rainfall evolution are displayed in Figure 4 a-c, after elimination of all synoptic and supra-synoptic time fluctuations (< 6 pentads or 30 days) by a high-pass butterworth filter (Murakami, 1979). Mean timing and duration of AP#1-3 are reproduced at the bottom diagrams. For example, the link between the AP#1 (which is from pentad 11 to 14) and each 5-day rainfall amount along the year is shown in Figure 4a. It clearly appears that the highest positive values ($> +0.7$ or $+0.9$) are always centered on these periods, suggesting both the important role of AP#1-3 for annual rainfall variability. For example, AP#1 is correlated with AP#3 over Sahel (Fig. 4a), whereas the Sudanian amounts during AP#2 and AP#3 periods are preceded by significant signals in February and March (Fig. 4b, c). The mean dates of AP occurrences are also depicted by the RR, H and LE signals in Figure 3 (look at the 1-5 mm/day, 40 and 80 W/m^2 lines in Fig. 3a, c, d respectively). Thus, from March to August, the successive APs could be controlled locally by the vertical fluxes of water and heat in a way where an enhanced hydrological cycle makes easier the AP generation. This arises the question of interannual variations in soil moisture availability during Spring and hence of the possible role of rainfall variations during monsoon withdrawal during the preceding Autumn.

IV. The role of wet and dry conditions during monsoon withdrawal

So monsoon conditions in northern Spring could be sensitive to the continental amounts registered during the preceding monsoon withdrawal independently from external and/or oceanic (SSTs) forcing. We illustrate first this statement through the soil moisture index (SWI) estimates provided by the ERS Scatterometer at a 10-day frequency for the period 1992-2000 (see section 2). The mean and abnormally wet and dry years SWI annual evolutions for the entire WAM region are presented in Figure 5. It is noteworthy that SWI values increases from the end of February to mid-September, lagging the rainfall cycle with a time delay of one month (compared with Fig. 1). However the dry curve reaches its

maximum before the wet one (first days of September against mid-September, respectively) and their synchronous differences are significant during Autumn.

Figure 6a shows the statistical impact of autumnal soil moisture variations registered over the Sudanian and Sahelian belts. It details, the relationship between September-December SWI anomalies in year 0 and soil moisture persistence in year +1 at a 10-day time-step and a sub-continental scale. The values are scaled in percentages of significant locations at $p=0.05$ regarding the wet minus dry SWI differences over 'Sudan-Sahel' relatively to the period 1992-2000 (wet: 1992, 93, 96, 97; dry: 1994, 95, 98, 99). So a value of 30% means that 30% of the 10,218 SWI Wet minus Dry differences (50km*50 Km) are locally significant. Notice first that the area significance exceeds largely the 5% threshold in Winter and reaches its maximum in March +1 ($> 30\%$), at the end of the dry season. At this time of the year (end of dry season) SWI is close to its annual minimum over the WAM region and over the Guinean and Sudanian belts. More generally, except a few small areas near the Guinean coast, the mean SWI field in March exhibits very low values (Fig. 6b). In March (Fig. 6c), the significant differences are largely positive, except for the sub-Saharan regions and some areas over the Nigeria (south of 10°N and east of 10°E); they tend to persist until June over the Sahelian band (shadings along 15°N in Fig. 6d). This 6-month persistence could change the initial conditions for the next monsoon season.

To study more directly and over a larger period the impacts of rains during monsoon withdrawal, we have done composite analysis relative to September-October (SO) rainfall (1979-2001). We define a year as WET (DRY) when the SO rainfall amounts are higher (lower) than the mean: the 10 wettest and 10 driest SO years are listed in table 1. Figure 7 shows the WET minus DRY (W-D) differences in 5-day rainfall and heat fluxes over a 21-month period (from January in year 0 to September in year +1). The results are tested locally using a paired Student t-test and globally (field significance) through 1000 Monte Carlo simulations.

The significant W-D rainfall estimates (Fig. 7a) concerns 8.8% of the data which is significant regarding field significance). After positive differences in September-October 0 over 'Sudan-Sahel' clear positive signals appear south of 10°N in March+1, July +1 and September+1 whereas months of May for both years (0 and +1) register negative W-D differences. These results show that rainfall amounts during monsoon withdrawal are statistically linked to the

timing and amplitude of precipitations during the next monsoon season. This might arise from changes in land surface (i.e., soil moisture and vegetation) since the H and LE differences (Fig. 7b, c) are clearly negative with H and positive with LE, according to variations in the H/LE Bowen ratio: the inverse H and LE behavior points to the role of variations in sensible versus latent partition of the net heat flux from the surface as a response to rainfall and soil wetness. Shinoda and Yamaguchi (2003) detail these processes over the Sahel through hourly soil moisture observations: basically increased (decreased) precipitation is accumulated as increased (decreased) soil moisture with a time lag, leading to decreased (increased) sensible heating and simultaneously increased (decreased) latent heating and finally to low (high) daily maximum temperature. The significant W-D signals at the $p=0.05$ level in Figures. 7b, c concern 12.7% and 20.7% of the H (negative differences) and LE (positive ones) diagrams, respectively. As for rainfall these panels are globally significant but the signals occur mainly from September 0 to March-April+1 over 'Sudan-Sahel' showing that before the rainy season, the sensible versus latent partition depends on local moisture availability.

Table 2 displays evolution of squared first rank autocorrelation coefficients (R^2) in the 5-day series as an estimate of simple time persistence (see the caption). It can be noticed that the highest values, centered on the months of November-February; are obtained with the heat fluxes ($R^2 > 40\%$) and vanish after May: since no rainfall occur in northern Winter, the H/LE partition depends directly on soil reservoir capacity and/or vegetation coverage. By contrast after the first rains these land surface parameters change locally and persistence decreases abruptly as shown in the Table.

The effect of soil moisture anomalies are logically more important in 'Sudan-Sahel' than near the Guinean coast, since over regions of low soil water content any small anomaly will change drastically the usual and will impact more the vegetation cover density. Figures 8 and 9 illustrate the statistical impacts of September-October rainfall variations over 'Sudan-Sahel' on the future active phases and pauses, and on soil moisture evolution, respectively. Curves in Figure 8 contrast precipitation following the most abnormally wet and dry withdrawal periods (SO) listed in table 1 for the entire WAM region (Fig. 8a), the 8°N - 12°N belt which exhibits a unique rainy season in Summer (Fig. 8b) and the 5°N - 7°N coastal area with two wet seasons in Spring and Autumn separated by a 'little dry season' in Summer (Fig. 8c). When wetter conditions occur at the end of the preceding rainy season one observes successively (1) more marked fluctuations in Spring with typically less rainfall in May but more in June (Fig. 8a, b),

(2) wetter rainy seasons in Summer (Fig. 8a, b), Spring and Autumn (Fig. 8c) along the Guinean coast where the little dry season occurs also in advance (by the end of July). By contrast, when SO precipitations of the preceding year are too rare, the rainy season is less abundant over the Sahelian and Sudanian belts; at the Guinean latitudes, the rainy seasons are also less abundant and separated by a marked little dry rainy season in August. Moreover, standard deviations of successive 5-day rainfall series extending from January to the end of August (the first 48 pentads in Fig. 8a-b) have been computed for the wet and dry cases: their mean values are significantly higher (lower) over WAM and Sudan-Sahel (8°N - 12°N) at $p=0.05$. So, even though not directly tested here, more (less) marked active phases and pauses after wet (dry) SO conditions are clearly observed in Figures. 8a, b.

Soil moisture evolutions over selected regions following abnormally wet and dry September-October rainfall variations (years underlined in Table 1) are shown in Figure 9: except over Guinea (Fig. 9d), positive W-D differences persist all along the dry season; they are mostly significant from September 0 to the end of April-May +1 over WAM and Sudan-Sahel (Fig. 9a,b). The wet curve (solid line in Fig. 9b) exhibits also higher -but not significant- SWI values in July-September +1. This relationship is also partly due to the fact that SWI is calculated by assuming an exponential decay using a soil and climate characteristic constant: at local scale Gaze et al. (1998) have shown from direct observations a rapid (2 months) depletion of soil moisture in the top 1 m of the soil. However, at regional scale, as shown in Figure 6, SWI persistence changes soil conditions during the dry season and hence the features of the future monsoon season.

V. Summary and Discussion

The general purpose of this study was to explore, through simple statistics, the possible control of rainfall fluctuations by an in-situ memory resulting from surface-atmosphere interactions over land, the other control being external forcing such as long-lived SST anomaly patterns. The first aim was to detect coherent signals at the surface-atmosphere interface through observed (CMAP data,) and modeled (NCEP/DOE reanalyses) heat and water vertical fluxes. The second one was to explain part of the link between abnormally wet soils in Fall using the Global Soil Moisture Archive from ERS Scatterometer and the next monsoon season and to document this long-term memory. We have then verified the hypothesis that active periods during the northern excursion of the WAM system are

sensitive to rainfall amounts registered at the beginning of the preceding monsoon withdrawal. Most of the results derive from data analyses at the 5-day after elimination of the synoptic and sub-synoptic variability (< 30 days), except for the soil moisture estimates which are at a 10-day frequency. They can be summarized as follows.

Over the WAM region the net total heat flux reaches a maximum in March-April due to the annual peak in its sensible component, it remains then nearly constant until the end of September due to the increasing latent flux component (Fig. 1). Even though clear heat flux and rainfall fluctuations exist in the supra-synoptic frequencies (13-16 and 20-25 day – periods), the most energetic signals are related to the intra-seasonal ones (30-90 days) (Figure. 2). The Spring to Summer period is marked by a maximum in sensible heat flux north of 10°N and a succession of active phases (APs with abrupt rainfall increases) (Fig.3). This is attested both in observations (CMAP, in situ rainfall not shown here) and in the NCEP reanalyzed vertical heat fluxes. A simple approach shows that APs tend to be concentrated on preferential short periods during the Spring to Summer installation of the monsoon (Fig. 1). There are four main AP periods: the turn of February/March at the Guinean latitudes (AP#1), mid-April (AP#2), then the end of May (AP#3) over the Guinean-Sudanian area and the turn of June/July (AP#4) for the Sudanian and Sahelian belts. APs #1-3 are significantly linked together (Fig. 4).

The results suggest also the existence of a “memory effect” triggered by preceding September-October rainfall anomalies. For example, composite analyses performed on the soil moisture index (SWI) estimates at a 10-day frequency (Fig. 5,6) show that rainfall excesses during monsoon withdrawal in year 0 generate positive soil moisture anomalies until the months of April and May +1 over the Sahelian and Sudanian belts, respectively. This relationship is partly due to the fact that local SWI values are calculated by assuming an exponential decay in time. However, at regional scale, the spatial extension of SWI significant anomalies reaches one maximum at the end of the dry season ($> 30\%$ of the West African continent in March +1): such an inter-seasonal persistence is able to change the horizontal energy gradients in low levels and hence to alter the initial conditions for the next West African monsoon season.

Figures 7-9 have shown that such soil moisture evolutions are sensitive to rainfall conditions in September-October during monsoon withdrawal. Such anomalies can affect significantly

the timing and amplitude of the next monsoon season (in year +1) even if part of monsoon variability responds to external and/or larger forcing, e.g. SST anomalies. Typically after the wettest conditions (i.e., abnormal rainfall excess in September-October) significant inverse anomalies occur in the sensible (negative values) and latent (positive) heat fluxes from September 0 to April +1 over 'Sudan-Sahel'. Higher (lower) intraseasonal variance in the 5-day rainfall January to August rainfall series is also observed after wet (dry) autumnal conditions, in coherency with more (less) marked active phases and pauses, along with: (1) Sahelian rainfall less (more) abundant in May (June); (2) wetter rainy seasons in Summer +1 at the Sahelian latitudes and in Spring and Autumn +1 along the Guinean coast where the 'little dry season' occurs in advance (at the end of July +1).

However, we have to mention that external forcing (teleconnections), long-lived SST anomaly patterns and vegetation cover have not been directly considered here. Part of the relationship involving soil moisture could also be due to the fact that local SWI values are calculated by assuming an exponential decay in time. Nonetheless, most of the preceding results are significant and have good internal consistency. They suggest that rainfall anomalies occurring at the end of the rainy season are of paramount importance for land-surface properties (soil, vegetation) during the dry season then in Spring and Summer for monsoon dynamics and precipitation. This arises yet the questions of (1) the capacity of semi-arid ecosystems to benefit from a water surplus at a multi-month lag, and of (2) the chain of processes linking these new surface parameters to monsoon dynamics. The first point has been recently investigated by Schwimning et al. (2004) and Martiny et al. (2005) using the Normalized Difference Vegetation Index (NDVI). These authors indicate first that clearly exists a memory of the past precipitation; second, they show that soil moisture favours increased seeds, production and more abundant foliar precession, whereas enhanced infiltration, decreased run-off and biogeochemical cycles facilitate vegetation growth.

The second question (forcing on monsoon dynamics in Spring) implies the existence of slow varying surface parameters (vegetation) at sub-continental scale and of more rapid feedbacks between soil moisture and the vertical fluxes at local scales. In fact large areas of vegetation cover (density, quality) change surface albedo and roughness but limit also direct evaporation and hence maintain humidity in low levels. Such a wetness excess exerts 2 types of forcing on the low troposphere: at local scale it strengthens the vertical moist static energy (MSE) gradients and thus the vertical instability; at regional scale it influences monsoon dynamics by

rearranging the horizontal MSE gradients (Emmanuel, 1995, Eltahir and Gong, 1996, Zheng and Eltahir, 1998 and Fontaine and Philippon, 2000) and associated rainfall amounts (Philippon and Fontaine, 2002). Although in a numerical model these gradients are not able to produce the observed structure of the African Easterly Jet (AEJ), as shown by Thorncroft and Blackburn (1999), they organize the monsoon flux and can contribute to the AEJ dynamics through temperature gradients magnified by meridional soil moisture gradients (Cook, 1999). In fact observations and atmospheric reanalyses show that (i) the relaxation of MSE gradients over land (southward orientated) in Spring is linked to the northward excursion of the system into the continent, and (ii) both the sensible-heating driven convection in low levels over the Sahel and the adiabatic ascents due to latent heat release in the high troposphere tend to reinforce before an abnormally wet rainy season (Fontaine et al., 2002).

So, the chain of processes at the end of the dry season could be as follows. (1) abnormally wetter soils in March (Fig. 6a, c) decrease surface albedo, but increase surface roughness, air moisture and low level convergence; (2) decreasing albedo reinforces locally the net solar radiation (so the upward radiation from the soil decreases) but lessens air temperature near the surface (so the boundary layer thickness diminishes); (3) the net surface radiation strengthens and therefore the surface-atmosphere heat flux. In the West African regional context this will reinforce MSE in low levels between the areas where soil moisture is abnormally high and the dry Sahara. Such a situation is favourable to monsoon circulation and to its northward penetration into the continent. In particular this will exert a differential forcing on the vertical atmospheric heating arrangement: the sensible flux will heat the near-surface layers whereas the latent flux will warm the atmosphere above the condensation level; this will impact monsoon dynamics at regional scale through the generation of horizontal thermal and moisture gradients and hence will affect both the amplitude and timing of precipitation.

Acknowledgements: The Authors are thankful to the American NOAA for providing the CMAP and NCEP/NCAR (National Center for Environmental Prediction and National Center for Atmospheric Research), data level II, and to the Global Precipitation Climatology Centre for additional rainfall estimates. They are thankful to the 2 anonymous reviewers for their very interesting suggestions and to Dr. S. Sijikumar to his careful reading of the manuscript. This work has been supported by the PNEDC and PNRH French programs (INSUE-CNRS) and is a contribution to the AMMA international project. *GPCC (1998): The Global Precipitation Climatology Centre. Information on World Wide Web under* <http://www.dwd.de/research/gpcc/>. Based on a French initiative, AMMA was built by an international scientific group and is currently funded by a large number of agencies, especially from France, UK, US and Africa. It has been the beneficiary of a major financial contribution from the European Community's Sixth Framework Research Programme. Detailed information on scientific coordination and funding is available on the AMMA International web site <http://www.amma-international.org>

REFERENCES

- Chang P, Li J and Li H (1997) A decadal climate variation in the tropical Atlantic Ocean from thermodynamic air-sea interactions. *Nature* 385: 516-518.
- Charney J, Quirk WJ, Show SH and Kornfield J (1975) Dynamics of deserts and droughts in the Sahel. *Quarterly Journal Of the Royal Meteorological Society* 101: 193-202.
- Charney JG, Quirk WJ, Show SH and Kornfield J. (1977) A comparative study of the effects of albedo change on drought in semiarid regions. *Journal of Atmospheric Science* 34: 1336-1385.
- Cook KH (1999) Generation of the African Easterly Jet and Its Role in Determining West African Precipitation. *Journal of Climate* 12: 1165-1184.
- Douville H and Chauvin F (2000) Relevance of soil moisture for seasonal climate predictions: a preliminary study. *Climate Dynamics* 16: 719-736.
- Eltahir EA and Gong C (1996) Dynamics of wet and dry years in West Africa, *Journal of Climate*. *Journal of Climate* 11: 2078-2096.
- Emanuel KA (1995) On thermally direct circulations in moist atmospheres. *Journal of Atmospheric Sciences* 52: 1529-1534.
- Folland CK, Palmer TN and Parker DE (1986) Sahel rainfall and worldwide sea temperature. *Nature* 320: 602-607.
- Fontaine B and Philippon N (2000) Seasonal evolution of boundary layer heat content in the West African monsoon from the NCEP/NCAR reanalysis (1968-1998). *International Journal of Climatology* 20: 1777-1790.
- Fontaine B, Philippon N and Camberlin P (1999) An improvement of June-September rainfall forecasting in the Sahel based upon region April-May moist static energy content (1968-1997). *Geophysical Research Letters* 26: 2041-2044.
- Fontaine B, Philippon N, Trzaska S and Roucou P (2002) Spring to Summer changes in the West African monsoon through NCEP/NCAR reanalyses (1968-1998). *Journal of Geophysical Research* 107 (10): 10.1029-10.1037.
- Gaze SR, Brouwer J, Simmonds LP and Bromley J (1998) Dry season water use patterns under *Guiera senegalensis* L. shrubs in a tropical savanna. *Journal of Arid Environments* 40: 53-67.
- Grodsky SA and Carton JA (2001) Coupled land/atmosphere interactions in the West African Monsoon. *Geophysical Research Letters* 28: 1503-1506.
- GPCC (1998): The Global Precipitation Climatology Centre. Information on World Wide Web under <http://www.dwd.de/research/gpcc/>

Janicot S and Sultan B (2001) Intra-seasonal modulation of convection in the West African monsoon. *Geophysical Research Letters* 28: 523-526.

Kanamitsu M, Ebisuzaki W, Woolen J, Yarg SK, Hnilo J J, Fiorino M and Potter GL (2002) NCEP-DOE AMIP-II reanalysis (R-2). *Bulletin of American Meteorological Society* 83: 1631-1643.

Li T and Philander SGH (1997) On the seasonal cycle of the equatorial Atlantic Ocean. *Journal of Climate* 10: 813-817.

Louvet S, Fontaine B and Roucou P (2003) Active phases and pauses during the installation of the West African monsoon through 5-day CMAP rainfall data (1979-2001). *Geophysical Research Letters* 30 (24): 2271-2275.

Louvet S and Janicot S (2003) Study of the first Guinean rainy season and role of the Subtropical Jet of the Northern Hemisphere. *Proceedings EGS-AGU Joint Assembly*.

Martiny N, Richard Y and Camberlin P (2005) Interannual persistence effects in vegetation dynamics of semi-arid Africa. *Geophysical Research Letters*, 32(24), L24403, doi:10.1029/2005GL024634, 2005.

Matthews AJ (2000) Propagation mechanisms for the Madden-Julian oscillation. *Quarterly Journal Of the Royal Meteorological Society* 126: 2637-2652.

Matthews AJ (2004) Intraseasonal variability over tropical Africa during northern summer. *Journal of Climate* 17: 2427-2440.

Maurer EP, O'Donnell GM and Lettenmaier DP (2001) Evaluation of the Land Surface Water Budget in NCEP/NCAR and NCEP/DOE Reanalyses using an Off-line Hydrologic Model. *Journal of Geophysical Research* 106 (D16): 17.841-17.862.

Mitchell TP and Wallace JM (1992) The annual cycle in equatorial convection and sea surface temperature. *Journal of Climate* 5: 1140-1156.

Murakami M (1979) Large scale aspects of deep convective activity over the Gate area. *Monthly Weather Review* 107: 994-1013.

Philippon N and Fontaine B (2002) The relationship between the Sahelian and previous 2nd Guinean rainy seasons: a monsoon regulation by soil wetness? *Annales Geophysicae* 20 (4): 575-582.

Schwinning S, Sala OE, Loik ME and Ehleringer JR (2004) Thresholds, memory, and seasonality: Understanding pulse dynamics in arid/semi-arid ecosystems. *Oecologia*: 191-193.

Shinoda M and Yamaguchi Y (2003) Influence of Soil Moisture Anomaly on Temperature in the Sahel: A Comparison between Wet and Dry Decades. *Journal of Hydrometeorology* 4 (2): 437-447.

Spencer RW (1993) Global oceanic precipitation from the MSU during 1979-91 and comparisons to other climatologies. *Journal of Climate* 6: 1301-1326.

Sultan B and Janicot S (2000) Abrupt shift of the ITCZ over West Africa and intra-seasonal variability. *Geophysical Research Letters* 27: 3353-3356.

Sultan B and Janicot S (2003) The West African Monsoon Dynamics. Part II : The "Preonset" and the "Onset" of the summer Monsoon. *Journal of Climate* 16: 3407-3427.

Sultan B, Janicot S and Diedhiou A. (2003) The West African Monsoon Dynamics. Part I : Documentation of Intra-seasonal variability. *Journal of Climate* 16 (21): 3389-3406.

Thorncroft CD and Blackburn M (1999) Maintenance of the African easterly jet. *Quarterly Journal Of the Royal Meteorological Society* 125: 763-786.

Wagner W, Lemoine G and Rott H (1999) A Method for Estimating Soil Moisture from ERS Scatterometer and Soil Data. *Remote Sens. Environ.*, 70: 191-207.

Wagner W and Scipal K (2000) Large-Scale Soil Moisture Mapping in Western Africa using the ERS Scatterometer, *IEEE Trans. IEEE Trans. Geosci. Remote Sensing* 38 (4): 1777-1783.

Wang G and Eltahir E (2000) Role of vegetation dynamics in enhancing the low-frequency variability of the Sahel rainfall. *Water resources research* 36: 1013-1021.

Xie P and Arkin PA (1997) Global precipitation: a 17-year monthly analysis based on gauge observations, satellite estimates, and numerical model outputs. *Bull. Amer. Meteor. Soc.* 78: 2539-2558.

Xue Y and Shukla J (1993) The influence of land surface properties on Sahel climate. Part I: Desertification. *Journal of Climate* 6: 2232-2245.

Zeng N, Neelin JD, Lau KM and Tucker C.J. (1999) Enhancement of interdecadal climate variability in the Sahel by vegetation interaction. *Science* 286: 1537-1540.

Zeng NJ and Neelin D (2000) The role of vegetation-climate interaction and interannual variability in shaping the African savanna. *Journal of Climate* 13: 2665-2670.

Zheng X and Eltahir EAB (1998) The role of vegetation in the dynamics of West African monsoons. *Journal of Climate* 11: 2078-2096.

TABLES

Table 1: The 10 most abnormally wet and dry September-October periods over the entire WAM domain and the Sahelian, Sudanian, Guinean belts defined in section 2 (1979-2001); underscores point out the years retained for the two-year evolution of SWI composites over 1992-2000.

Wet Sep-Oct periods	WAM: 1979 1980 1981 1984 1986 1987 1988 1989 <u>1994 1998</u>
	SUD-SAH : 1979 1981 1984 1986 1988 <u>1994 1995</u> 1996 <u>1998 1999</u>
	SAH: 1979 1980 1984 1986 1994 1995 1996 1997 1998 1999
	SUD: 1979 1981 1984 1986 1988 1994 1995 1998 1999
	GUI: 1979 1980 1981 1982 1984 1987 1988 1989 <u>1994 1995</u>
Dry Sep-Oct periods	WAM: 1983 1985 1990 1991 <u>1992 1993 1996 1997</u> 1999 2001
	SUD-SAH: 1982 1983 1985 1990 1991 <u>1992 1993 1997</u> 2000 2001
	SAH: 1982 1983 1985 1987 1988 1989 1990 1991 1992 2001
	SUD: 1982 1983 1985 1990 1991 1992 1993 1997 2000 2001
	GUI: 1983 1985 1990 1991 <u>1992 1996 1997 1999</u> 2000 2001

Table 2: Squared first rank autocorrelation coefficients (R²) computed on the raw 5-day RR, H, LE and H/LE time series averaged over the 5°N-12°N Sudanian-Guinean belt for different bimonthly periods. Each time series corresponds to the successive 5-day raw (non filtered) values selected over a 2-month period (i.e., the JF time series corresponds to the first twelve pentad values of each year (23 years), hence to all the 12*23 January-February pentads; the MA series corresponds to the pentad numbers 13 to 24 of each year...). Asters mark the significant values at the p=0.05 level taking into account the equivalent number of degrees of freedom in the series. Period 1979-2001.

5N-12N	JF	MA	MJ	JA	SO	ND
RR	04	18	11	10	42*	23
H	59*	38*	39*	28	52*	41*
LE	47*	33	09	04	07	57*
H/LE	70*	50*	36	29	56*	53*

CAPTIONS

Figure 1: Left (a,d,g) Mean Sahelian annual evolutions (1979-2001) of filtered rainfall records (curve and error-bars) in mm/day after elimination of synoptic and supra-synoptic fluctuations (< 5 pentads); middle (b,e,h) rainfall tendencies (differences between successive pentads) in mm/day; right (c,f,i), the sensible (H, dashed line), latent (LE, thin line) and total (H+LE, bold line) net heat fluxes at the surface (curves) in W/m^2 bands at a 5-day time-step. The black bars in b,e,h mark the beginning of rainfall changes observed at least in 2/3 of years with an absolute difference $> +/- 0.05$ mm/day between 3 successive pentads.

(c,d) for the Sudanian belt with rainfall changes $> +/- 0.18$ mm/day;

(e,f) for the Guinean belt with rainfall changes $> +/- 0.21$ mm/day.

Figure 2: (a) Power spectral density estimates of the detrended 5-day rainfall anomaly time series averaged over the Sahelian belt after elimination of variations linked to the mean annual cycle (annual and semi-annual periods) and inter-annual scales by a low-pass butterworth filter (< 30 pentads, 150 days). Asters mark the significant peaks regarding a Monte Carlo procedure (1000 random rank permutations in the series). Period 1979-2001.

(b): as (a) but for the Sudanian belt;

(c): as (a) but for the Guinean belt.

Figure 3: (a): Mean annual evolutions of continental rainfall in mm/day over the WAM domain ($5^{\circ}N-20^{\circ}N$; $10^{\circ}W-10^{\circ}E$) as a function of latitudes, after elimination of all fluctuations < 30 days. Maximums are shaded. Period 1979-2001.

(b) as above but for the total heat flux in W/m^2

(c) as above but for the sensible heat flux in W/m^2

(d) as above but for the latent heat flux in W/m^2

Figure 4: (a) Correlation coefficients between time series of rainfall amounts registered averaged over a given latitude during the first active period (AP#1) and the successive 5-day rainfall amounts along the years (73 pentads each year) as a function of time and latitudes, after elimination of fluctuations < 30 days (see text). Period 1979-2001.

(b) as above but for the second active period (AP#2);

(c) as above but for the third active period (AP#3).

Figure 5: (a) Interannual evolution of the ERS soil water index (SWI) averaged over WAM.

(b) Mean (solid bold), wet (solid) and dry (dashed) annual evolutions. The differences are tested using a paired Student t-test at $p=0.05$ with negative (positive) differences in dashed (solid) lines; asters for significant values. Period 1992-2000.

Figure 6: Typical results regarding the ERS soil water index (SWI) evolution.

(a): Annual evolution at a 10- day time-step of percentages of significant areas over the West African continent (period 1992-2000).

(b): Mean SWI field in March;

(c,d) Significant wet minus dry SWI differences in March (c) and June (d) regarding the abnormally wet and dry September-December periods over 'Sudan-Sahel' (see Table 1). The Wet minus Dry differences are tested using a paired Student t-test at $p=0.05$.

Figure 7: (a) wet minus dry rainfall differences over a 19 month period (January0 to September+1) regarding the 10 wettest and 10 driest yearly rainfall amounts averaged over the WAM region. Local differences are tested using a paired Student t-test at $p=0.05$ with negative (positive) differences in dashed (solid) lines, and significant values in grey. Field significances at $p=0.05$ and 0.01 , respectively 6.82% and 8.14%, are evaluated using Monte Carlo procedures in which the wet versus dry correspondences are shuffled randomly 1000 times. Period 1979-2001.

(b) As above but for the sensible heat flux; field significances at $p=0.05$ and 0.01 are respectively 9.06% and 11.55%.

(c) As above but for the latent heat flux; field significances at $p=0.05$ and 0.01 are respectively 9.58% and 12.60%.

Figure 8: (a) Annual evolution of rainfall following the abnormally wet (solid line) and dry (dashed line) withdrawal periods (SO) over 'Sudan-Sahel' (see selected years in Table 1) for the WAM domain. The differences are tested using a paired Student t-test at $p=0.05$ with negative (positive) differences in dashed (solid) lines, and significant values marked by asters. Period 1979-2001.

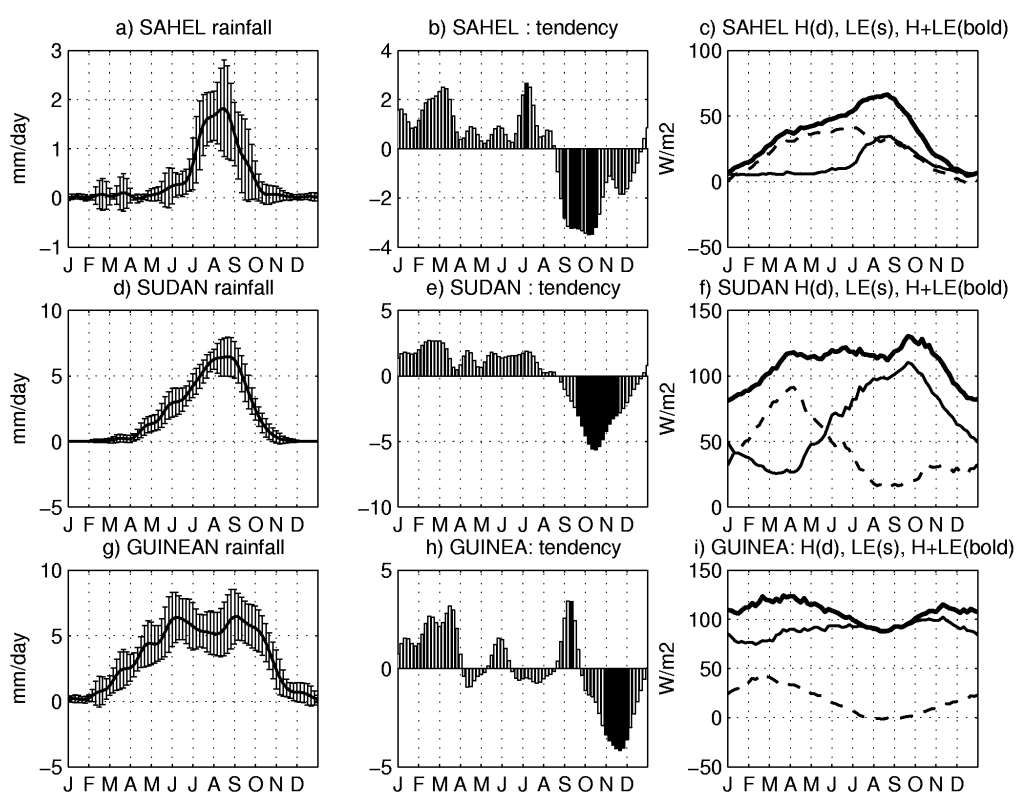
(b) for the 12°N-8°N belt;

(c) for the coastal Guinean region (5°N-7°N).

Figure 9: (a) Composites of the ERS soil water index averaged (SWI) over the WAM region regarding the preceding abnormally wet (solid line) and dry (dashed line) withdrawal periods (SOND) over 'Sudan-Sahel' defined in Table 1. The Wet minus Dry differences are tested using a paired Student t-test at $p=0.05$ with significant values marked by asters. Period 1992-2000.

(b) as above but for the Sudan-Sahel belt

(c) as above but for the Guinean belt



*

Figure 1: Left (a,d,g) Mean Sahelian annual evolutions (1979-2001) of filtered rainfall records (curve and error-bars) in mm/day after elimination of synoptic and supra-synoptic fluctuations (< 5 pentads); middle (b,e,h) rainfall tendencies (differences between successive pentads) in mm/day; right (c,f,i), the sensible (H, dashed line), latent (LE, thin line) and total (H+LE, bold line) net heat fluxes at the surface (curves) in W/m^2 bands at a 5-day time-step. The black bars in b,e,h mark the beginning of rainfall changes observed at least in 2/3 of years with an absolute difference $> +/- 0.05$ mm/day between 3 successive pentads.

(c,d) for the Sudanian belt with rainfall changes $> +/- 0.18$ mm/day;

(e,f) for the Guinean belt with rainfall changes $> +/- 0.21$ mm/day.

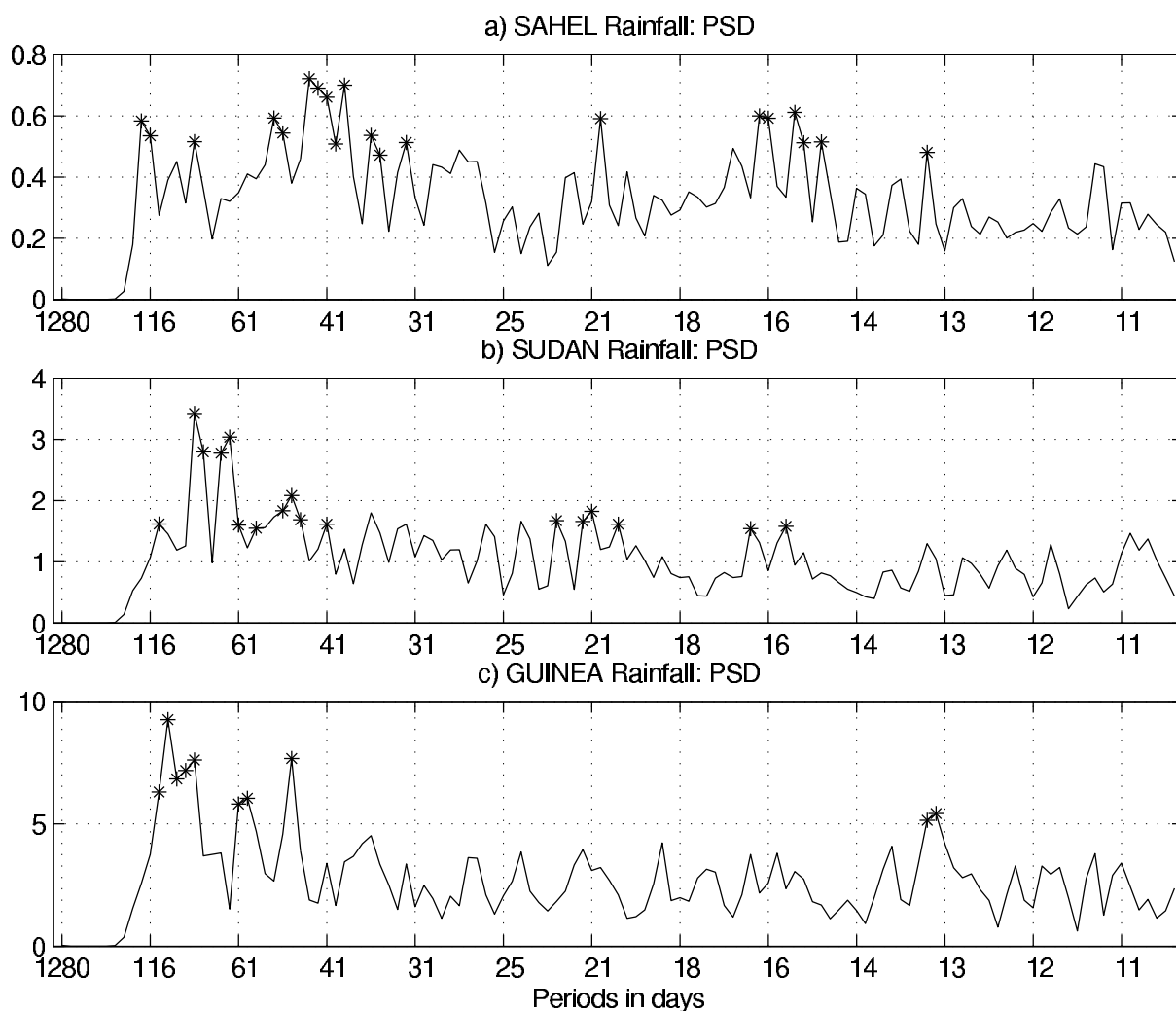


Figure 2: (a) Power spectral density estimates of the detrended 5-day rainfall anomaly time series averaged over the Sahelian belt after elimination of variations linked to the mean annual cycle (annual and semi-annual periods) and inter-annual scales by a low-pass butterworth filter (< 30 pentads, 150 days). Asterisks mark the significant peaks regarding a Monte Carlo procedure (1000 random rank permutations in the series). Period 1979-2001.

(b): as (a) but for the Sudanian belt;

(c): as (a) but for the Guinean belt.

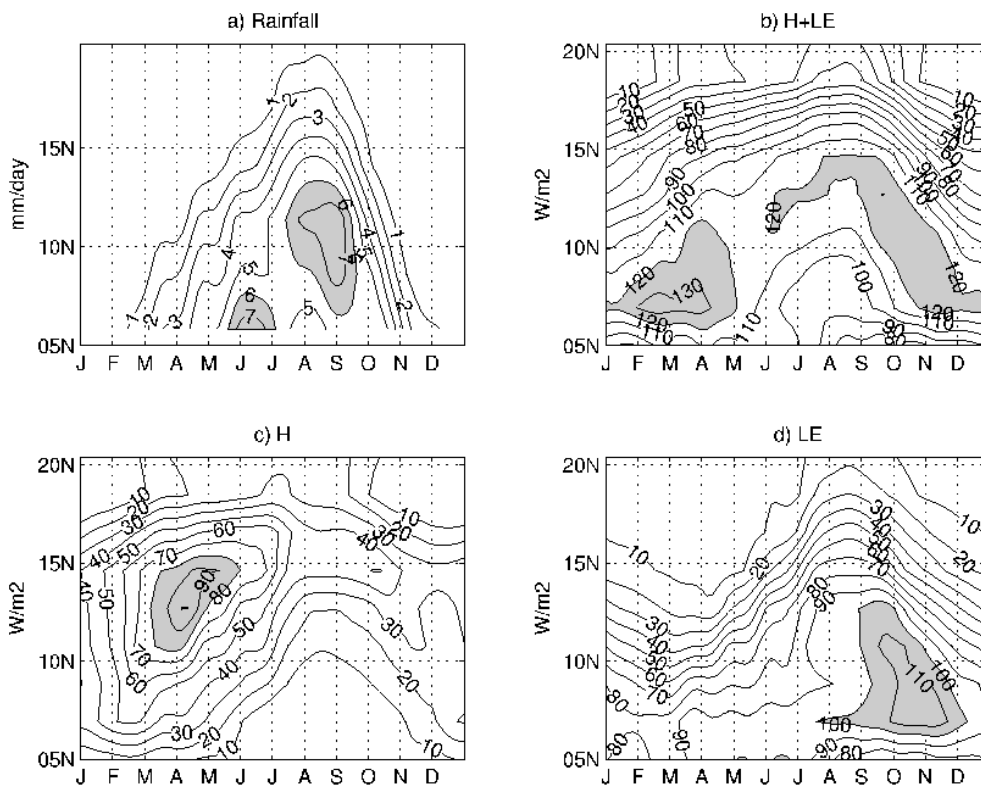


Figure 3: (a): Mean annual evolutions of continental rainfall in mm/day over the WAM domain (5°N-20°N; 10°W-10°E) as a function of latitudes, after elimination of all fluctuations < 30 days. Maximums are shaded. Period 1979-2001.

- (b) as above but for the total heat flux in W/m^2
- (c) as above but for the sensible heat flux in W/m^2
- (e) as above but for the latent heat flux in W/m^2

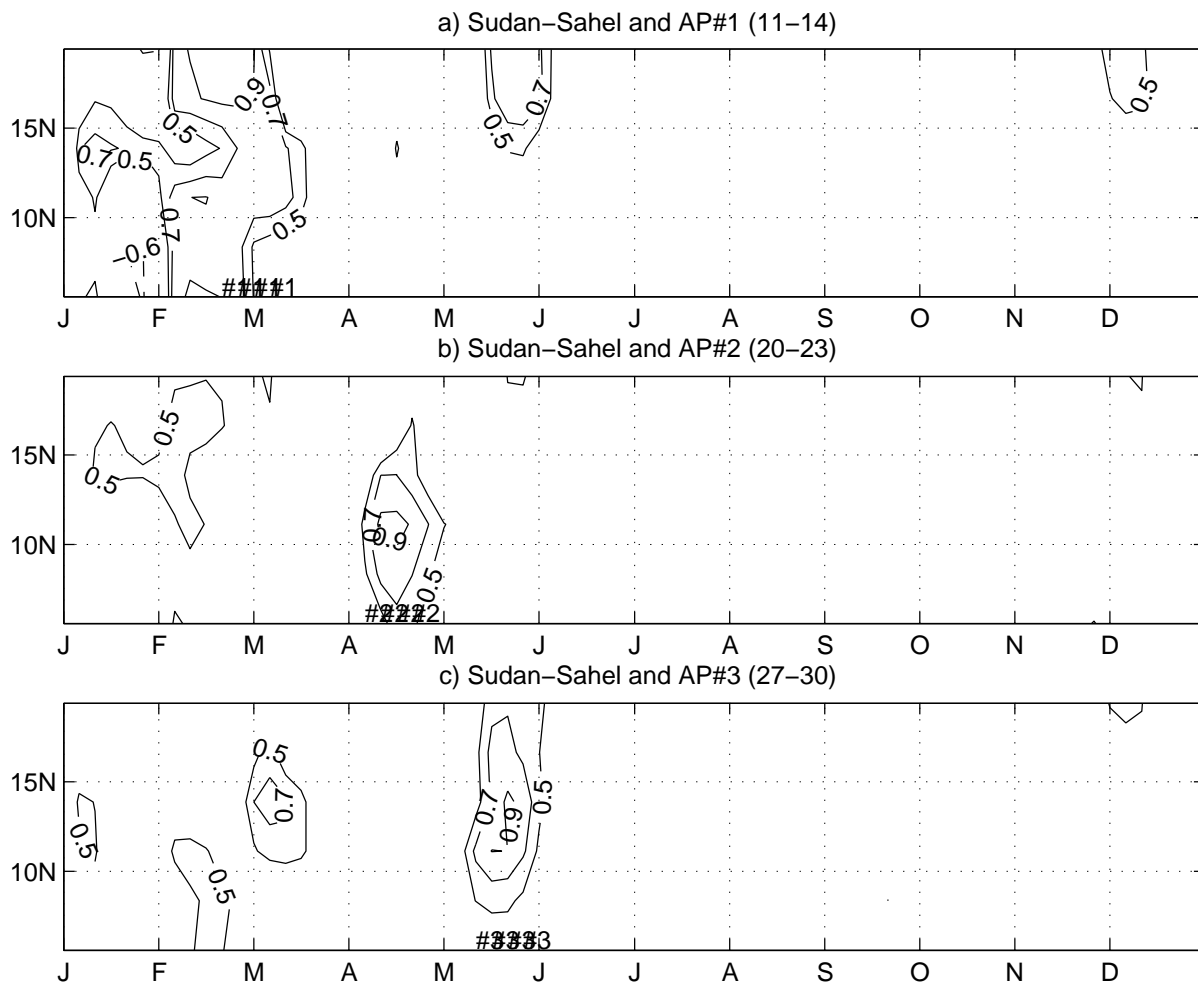


Figure 4: (a) Correlation coefficients between time series of rainfall amounts registered averaged over a given latitude during the first active period (AP#1) and the successive 5-day rainfall amounts along the years (73 pentads each year) as a function of time and latitudes, after elimination of fluctuations < 30 days (see text). Period 1979-2001.

- (b) as above but for the second active period (AP#2);
- (c) as above but for the third active period (AP#3).

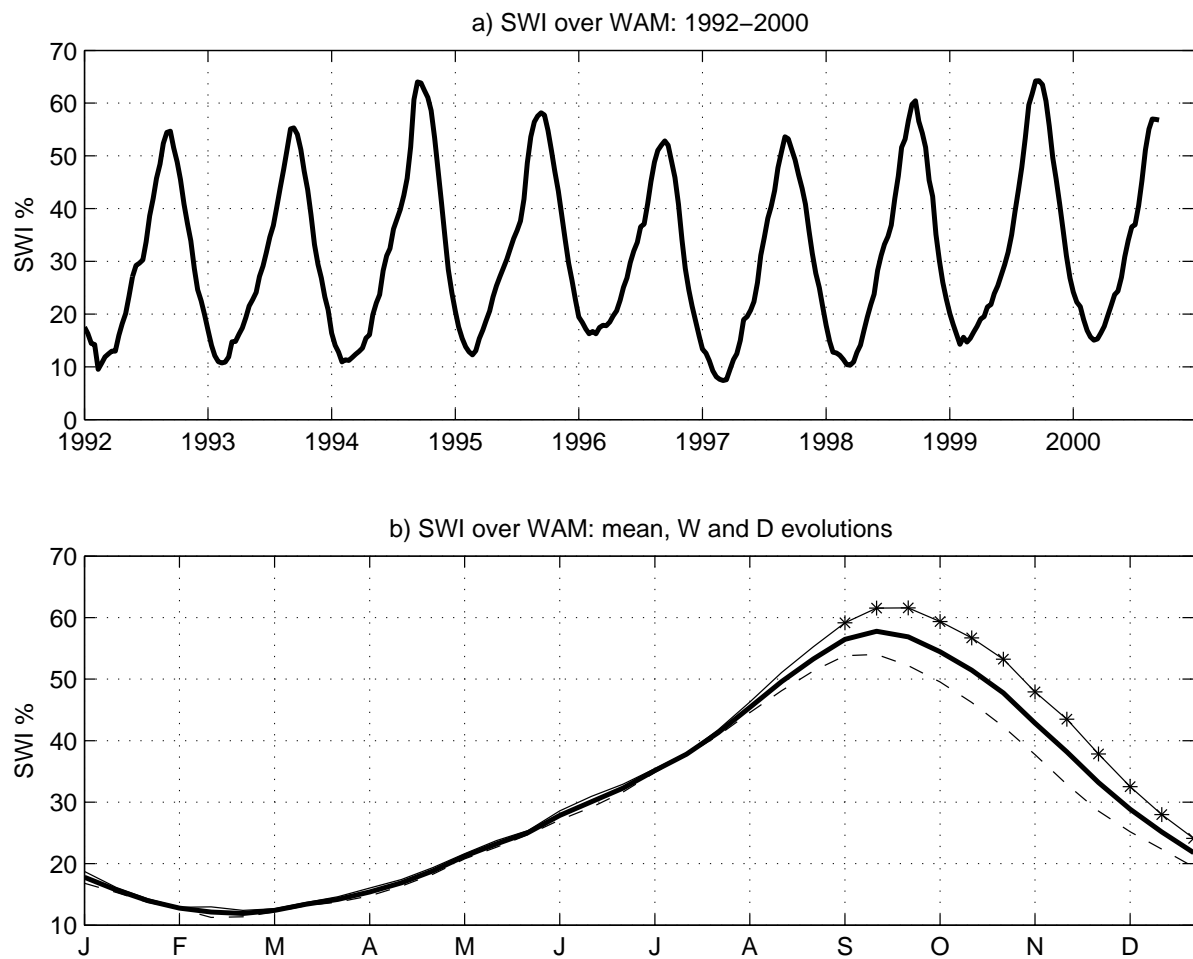


Figure 5: (a) Interannual evolution of the ERS soil water index (SWI) averaged over WAM.

(b) Mean (solid bold), wet (solid) and dry (dashed) annual evolutions. The differences are tested using a paired Student t-test at $p=0.05$ with negative (positive) differences in dashed (solid) lines; asters for significant values. Period 1992-2000.

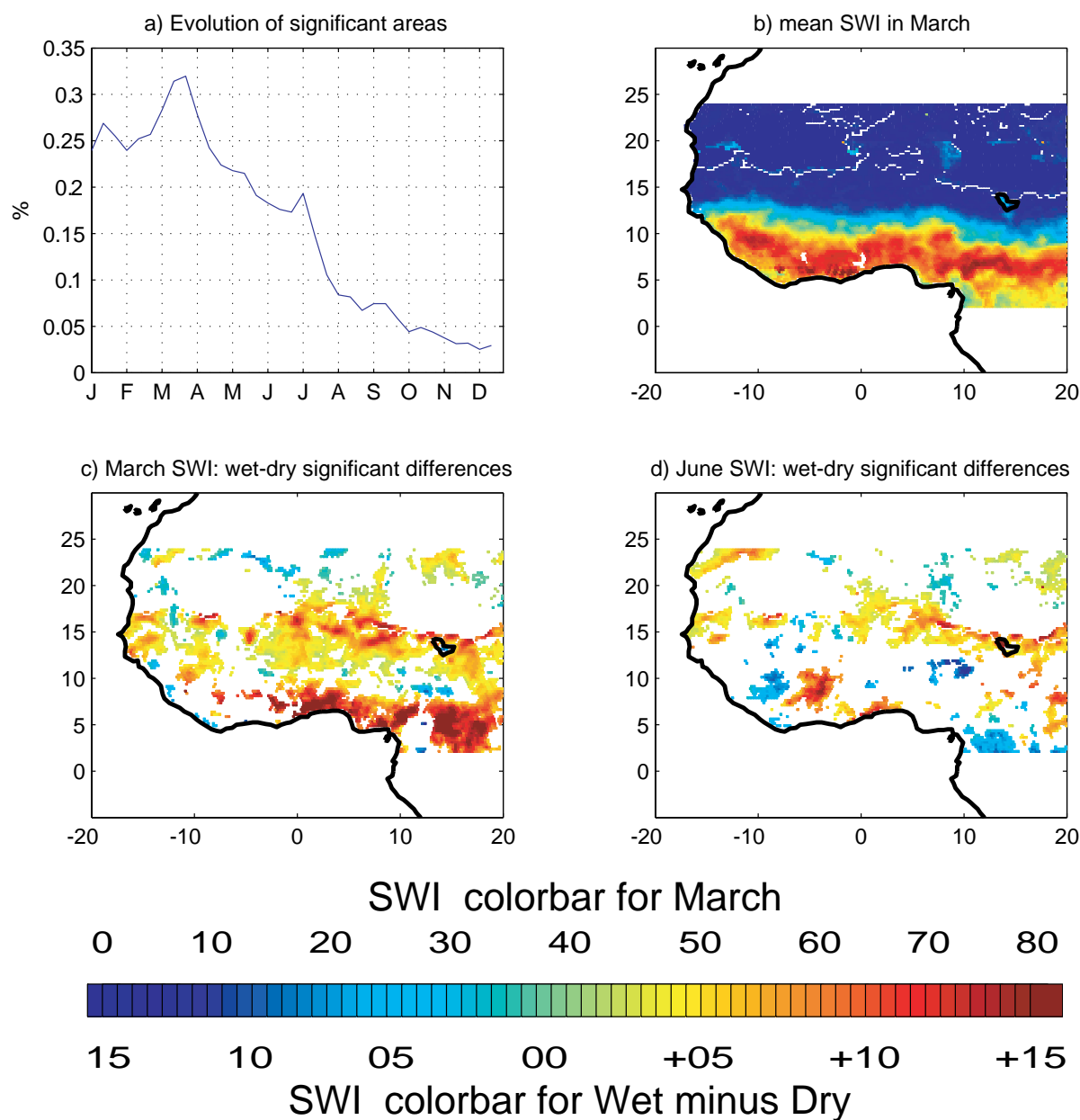


Figure 6: Typical results regarding the ERS soil water index (SWI) evolution.

(a): Annual evolution at a 10- day time-step of percentages of significant areas over the West African continent (period 1992-2000).

(b): Mean SWI field in March;

(c,d) Significant wet minus dry SWI differences in March (c) and June (d) regarding the abnormally wet and dry September-December periods over ‘Sudan-Sahel’ (see Table 1). The Wet minus Dry differences are tested using a paired Student t-test at $p=0.05$.

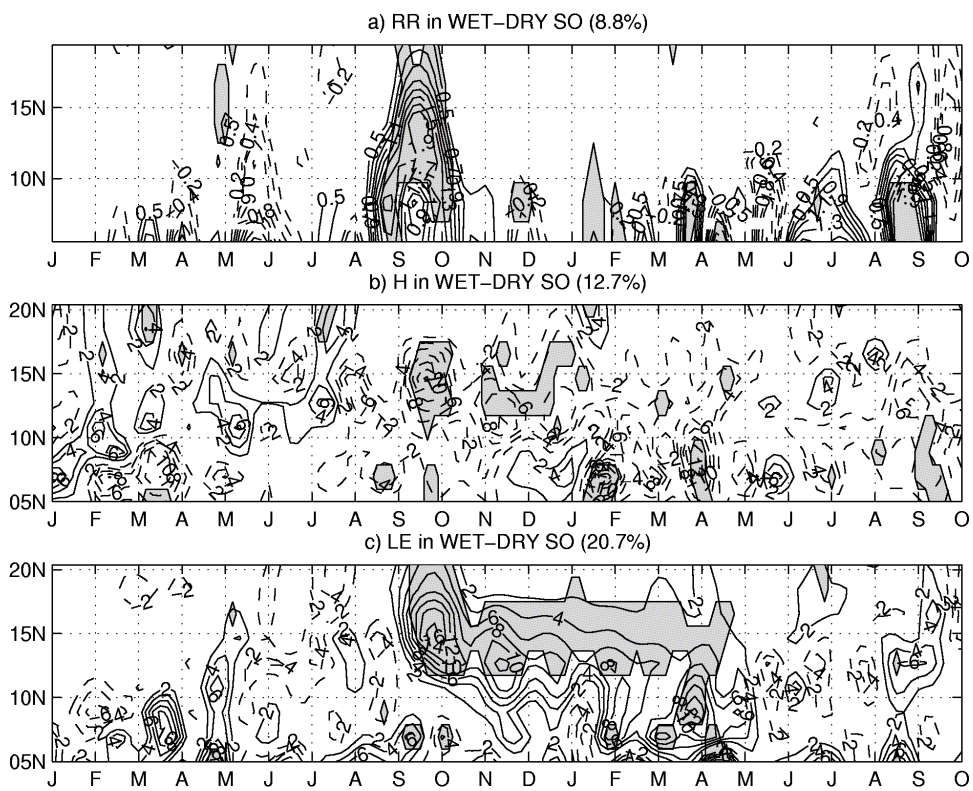


Figure 7: (a) wet minus dry rainfall differences over a 19 month period (January0 to September+1) regarding the 10 wettest and 10 driest yearly rainfall amounts averaged over the WAM region. Local differences are tested using a paired Student t-test at $p=0.05$ with negative (positive) differences in dashed (solid) lines, and significant values in grey. Field significances at $p=0.05$ and 0.01 , respectively 6.82% and 8.14%, are evaluated using Monte Carlo procedures in which the wet versus dry correspondences are shuffled randomly 1000 times. Period 1979-2001.

(b) As above but for the sensible heat flux; field significances at $p=0.05$ and 0.01 are respectively 9.06% and 11.55%.

(c) As above but for the latent heat flux; field significances at $p=0.05$ and 0.01 are respectively 9.58% and 12.60%.

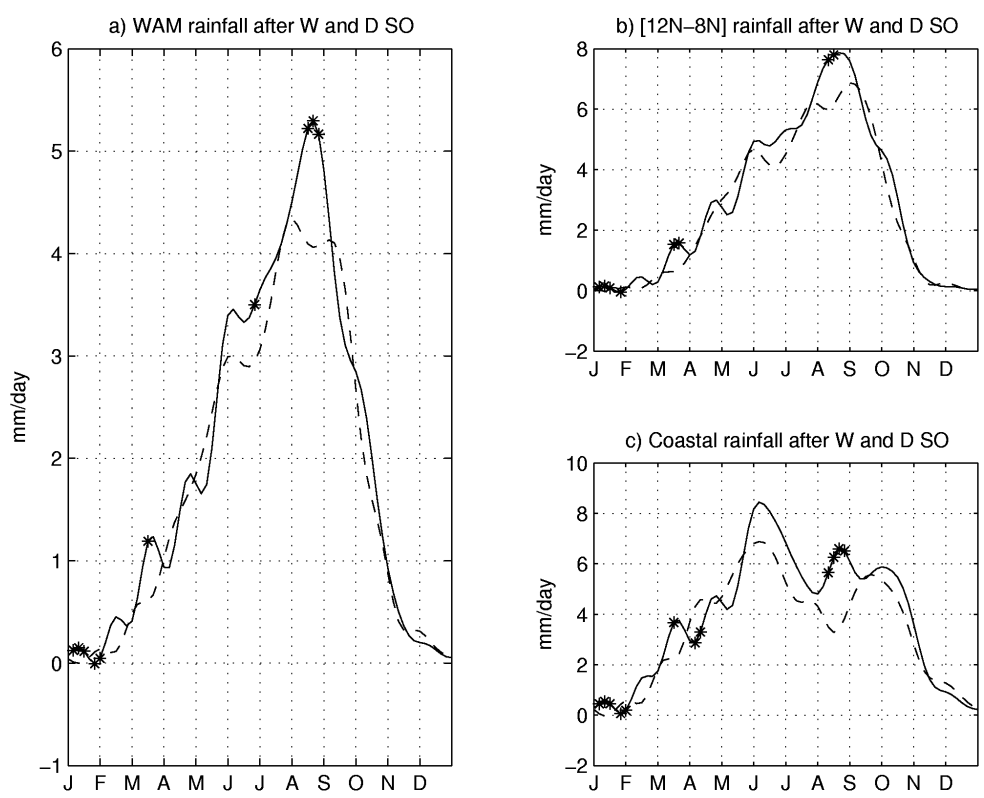


Figure 8: (a) Annual evolution of rainfall following the abnormally wet (solid line) and dry (dashed line) withdrawal periods (SO) over ‘Sudan-Sahel’ (see selected years in Table 1)

for the WAM domain. The differences are tested using a paired Student t-test at $p=0.05$ with negative (positive) differences in dashed (solid) lines, and significant values marked by asters. Period 1979-2001.

(b) for the 12°N - 8°N belt;

(c) for the coastal Guinean region (5°N - 7°N).

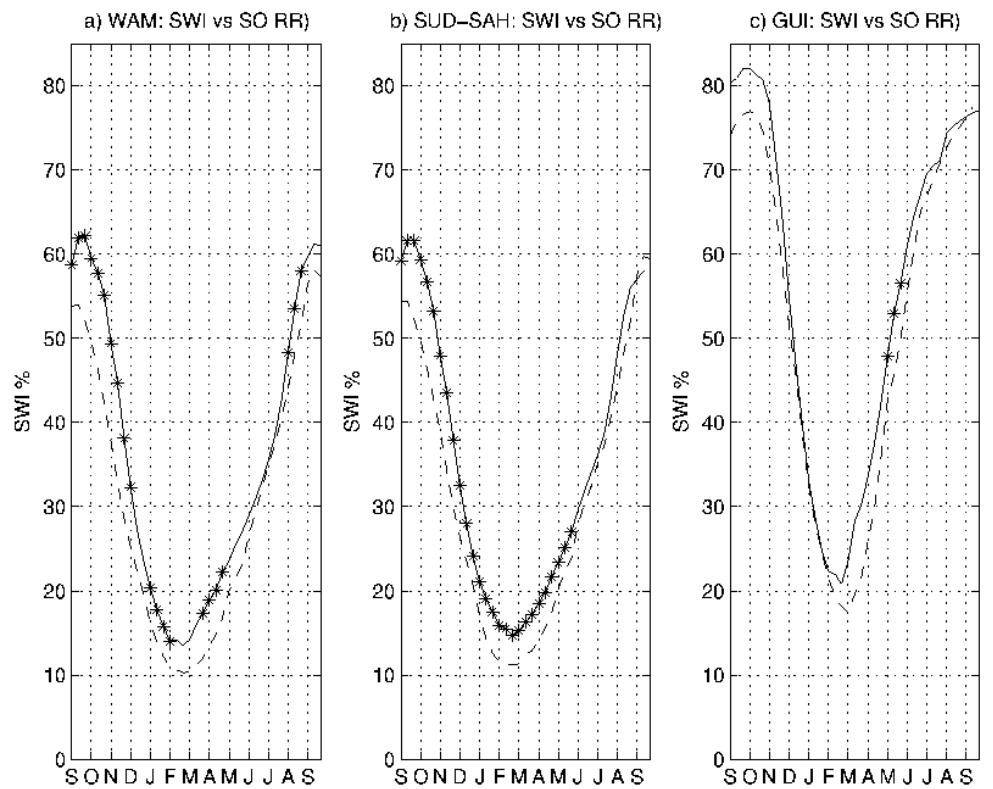


Figure 9: (a) Composites of the ERS soil water index averaged (SWI) over the WAM region regarding the preceding abnormally wet (solid line) and dry (dashed line) withdrawal

periods (SOND) over 'Sudan-Sahel' defined in Table 1. The Wet minus Dry differences are tested using a paired Student t-test at $p=0.05$ with significant values marked by asters. Period 1992-2000.

(b) as above but for the Sudan-Sahel belt

(c) as above but for the Guinean belt